Title

Divalent regulation and intersubunit interactions of human Connexin26 (Cx26) hemichannels

Journal

Channels, 8(1)

ISSN

1933-6950

Authors

Lopez, William
Liu, Yu
Harris, Andrew L
et al.

Publication Date

2014

DOI

10.4161/chan.26789

Peer reviewed

Channels 8:1, 1–4; January/February 2014; © 2014 Landes Bioscience

Divalent regulation and intersubunit interactions of human Connexin26 (Cx26) hemichannels

William Lopez, Yu Liu, Andrew L Harris, and Jorge E Contreras*

Department of Pharmacology and Physiology; New Jersey Medical School; Rutgers University; Newark, NJ USA

Control of plasma membrane connexin hemichannel opening is indispensable, and is achieved by physiological extracellular divalent ion concentrations. Here, we explore the differences between regulation by Ca^{2+} and Mg^{2+} of human connexin26 (hCx26) hemichannels and the role of a specific interaction in regulation by Ca^{2+}. To effect hemichannel closure, the apparent affinity of Ca^{2+} (0.33 mM) is higher than for Mg^{2+} (1.8 mM). Hemichannel closure is accelerated by physiological Ca^{2+} concentrations, but non-physiological concentrations of extracellular Mg^{2+} are required for this effect. Our recent report provided evidence that extracellular Ca^{2+} facilitates hCx26 hemichannel closing by disrupting a salt bridge interaction between positions D50 and K61 that stabilizes the open state. New evidence from mutant cycle analysis indicates that D50 also interacts with Q48. We find that the D50-Q48 interaction contributes to stabilization of the open state, but that it is relatively insensitive to disruption by extracellular Ca^{2+} compared with the D50-K61 interaction.

Keywords: Connexin, gating, calcium, salt bridge, channelopathies

*Correspondence to: Jorge E Contreras; Email: contrejo@njms.rutgers.edu

Submitted: 09/10/2013

Revised: 10/11/2013

Accepted: 10/11/2013

Published Online: 10/14/2013

http://dx.doi.org/10.4161/chan.26789

Commentary to: Lopez W, Gonzalez J, Liu Y, Harris AL, Contreras JE. Insights on the mechanisms of Ca(2+) regulation of connexin26 hemichannels revealed by human pathogenic mutations (D50N/Y). J Gen Physiol 2013; 142:23–35; PMID:23797420; http://dx.doi.org/10.1085/jgp.201210893

Introduction

Connexins constitute a family of transmembrane proteins, with 20 members in humans, which are expressed in almost all cellular types.[1] At the molecular level, connexins assemble as hexamers to form hemichannels. Hemichannels are transported to the plasma membrane, where most dock with hemichannels in apposed cells to form gap junction channels (GJCs).[2] GJCs allow propagation of electrical and/or molecular signaling among neighboring cells by direct intercellular communication.[3] Unpaired hemichannels, those not forming GJCs, seem to play an autocrine/paracrine role by releasing transmitters, such as glutamate and ATP, into the extracellular medium. Several connexin mutations that cause human disease result in dysfunction of hemichannel regulation by extracellular Ca^{2+}.[4,5] A molecular and mechanistic understanding of Ca^{2+} regulation of hemichannel gating will help to elucidate how these mutations produce connexin channelopathies.

Result and Discussion

We assessed connexin hemichannel activation and deactivation in oocytes expressing hCx26 protein using the 2-electrode voltage-clamp technique. The peak tail currents and their relaxation kinetics following a depolarizing pulse from -80 to 0 mV were examined. Using this protocol, we previously showed that the peak tail currents increase with reduction of external divalent ions. **Figure 1A** shows current traces obtained at 1.8, 0.5, and 0.01 mM extracellular Ca^{2+} and Mg^{2+} from 2 different oocytes expressing moderate levels of hCx26 currents. The peak tail currents are reduced with increased external Ca^{2+}, showing that external Ca^{2+} inhibits activation of hCx26 hemichannels, as previously shown.[6] By comparison, the same concentrations of extracellular Mg^{2+} are much less effective in reducing the tail currents. Consistent

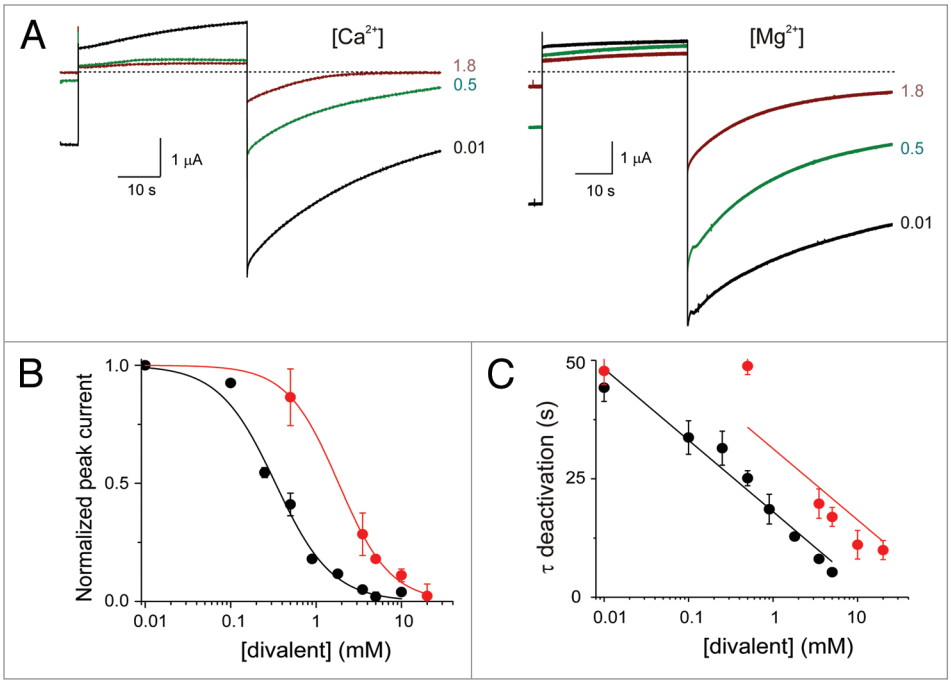

Figure 1. Ca^{2+}, but not Mg^{2+}, is the main physiological divalent regulator of hCx26 hemichannels. (**A**) Current traces elicited by a voltage pulse from -80 to 0 mV from oocytes expressing hCx26 hemichannels in the presence of the indicated Ca^{2+} (right panel) or Mg^{2+} (left panel) concentrations (in mM). (**B**) Dose-response relation for Ca^{2+} (black) or Mg^{2+} (red) determined from the peak tail currents following voltage pulses from -80 to 0 mV. The solid line represents the best fit of the data to a Hill equation (**Eq. 1**). (**C**) Deactivation time constants as a function of Ca^{2+} (black) or Mg^{2+} (red) concentrations. The solid lines correspond to linear fits to the data. The data points represent mean ± SEM of at least 3 independent measurements.

with this observation, the holding currents prior to depolarization are significantly decreased in the presence of Ca^{2+} compared with those in the presence of Mg^{2+}. These results suggest that Mg^{2+} does not efficiently close hemichannels even at -80 mV.

Figure 1B shows the dose-response relations for normalized hemichannel tail currents. The data are fit to a Hill equation of the form: $I/I_{max} = 1/[1+([X^{2+}]/K_D)^n]$ **(Eq. 1)**, where the divalent ion concentration is $[X^{2+}]$, the fractional current is I/I_{max}, I is the tail current at a particular divalent ion concentration, I_{max} is the maximal tail current activation at 0.01 mM divalent ion, K_D is the apparent affinity and *n* is the Hill coefficient. The calculated values for the apparent K_D for inhibition of hCx26 hemichannels by extracellular Ca^{2+} and Mg^{2+} are 0.33 mM and 1.8 mM, respectively. The best-fit parameter values for *n* are about 1.38 and 1.41 for extracellular Ca^{2+} and Mg^{2+}, respectively. At physiological Ca^{2+} concentrations (1.0 – 2.0 mM), hCx26 hemichannels are ≤ 15% of the maximal activation, but at the corresponding Mg^{2+} concentrations they are ≥ 50% of the maximal activation.

Figure 1C shows the deactivation time constants of the tail currents as a function of Ca^{2+} and Mg^{2+}. Deactivation kinetics are dramatically accelerated by Ca^{2+} concentrations from 0.01 to 5.0 mM. In contrast, Mg^{2+} starts to accelerate the closure only above 0.5 mM, and the effect is much less. The steady-state and kinetic data support the idea that, under physiological ionic conditions, extracellular Ca^{2+}, but not extracellular Mg^{2+}, plays a major role stabilizing and facilitating closing of Cx26 hemichannels.

We previously showed that the Ca^{2+}-dependent closing kinetics of hCx26 hemichannels are mostly mediated by disruption of an electrostatic interaction between positions D50 and K61 that stabilizes the open state.[6] Double mutant cycle analyses support a thermodynamic linkage between Ca^{2+} and disruption of the D50-K61 interaction in open channels. In addition, single disease-causing mutations at position D50(N/Y) eliminate Ca^{2+} sensitivity of the hemichannel currents and accelerate deactivation kinetics, supporting the idea that in open wild-type hemichannels D50 forms an electrostatic interaction with K61 that is disrupted by external Ca^{2+}.

Consistent with these data, we observed that substitution of D50 with an alanine (D50A mutation) accelerates hemichannel closure as reflected in the deactivation time constants of tail currents in response to depolarizing pulses from -80 to 0 mV and essentially eliminates their Ca^{2+} dependences (**Fig. 2A**, upper, and orange data points in **Fig. 2B**). This further supports the notion that the lack of a negative charge at position D50 mimics disruption of a D50-K61 salt bridge by Ca^{2+}.

Interestingly, a recently revised version of the hCx26 GJC crystal structure supports an inter-subunit interaction between positions D50 and K61 at a distance of 2.8 Å, and also suggests that D50 forms an inter-subunit interaction with position Q48.[7,8] A recent study using mutation and cysteine cross-linkages further supports a functional interaction between Q48 and D50,[8] but the contribution of this interaction to the Ca^{2+} sensitivity of hCx26 hemichannel closure was not clear. For this reason, we tested the effect of this interaction on the Ca^{2+} dependence of the deactivation time constants by substituting an alanine residue at position 48 (Q48A mutation). **Figure 2A** (lower) shows current traces in response to depolarizing pulses from -80 to 0 mV in the presence 0.1, 0.5, and 1.8 mM Ca^{2+} for an oocyte expressing Q48A. The holding currents and peak tail currents increase as extracellular Ca^{2+} is reduced. At 1.8 mM Ca^{2+}, the deactivation kinetics display 2 components, a fast component of 1.6 ± 0.5 s and a slow component of 10 ± 0.4 s, the latter being similar to the wild-type behavior. **Figure 2B** (green) shows the Ca^{2+} sensitivity of the rate-limiting slow component. In contrast to the D50A mutant, the deactivation kinetics (hemichannel closure) of the Q48A

hemichannels are only slightly increased at low Ca^{2+} concentrations (below 0.1 mM), but are markedly more rapid, compared with the wild-type channels, at higher Ca^{2+} concentrations. Thus, mutation at Q48 suggests that, in wild-type channels, Q48 plays a role in stabilizing the open state of hCx26 hemichannels, but its stabilizing effect is less than that of the charge at D50 (i.e., it is insensitive to the Ca^{2+} concentration below 0.2 mM, and above that level the deactivation is more rapid than wild-type, but slower than for the D50 mutant). The implication is that the effect of Ca^{2+} that involves Q48 is a lesser component of the overall Ca^{2+} sensitivity than are the interactions of D50 with other residues (e.g., with K61).

To investigate the Ca^{2+}-dependent coupling energy between residues D50 and Q48, we performed double mutant cycle analysis using apparent affinities for Ca^{2+} from wild-type, Q48A and D50A single mutants, and D50A/Q48A double mutant channels. **Figure 3A** shows the $[Ca^{2+}]$ dose-response relations for wild-type and mutant channels. The calculated values for K_D are 0.33, 0.15, 0.75, and 1.7 mM for wild-type, Q48A and D50A single mutants, and D50A/Q48A double mutant channels, respectively. The pairwise interaction energy between positions D50 and Q48 was estimated using **Equation 2** (see Methods). This analysis yielded a coupling energy ($\Delta\Delta G$) of - 0.63 kcal/mol (the cut off for non-specific interaction is below ± 0.5 kcal/mol). Strikingly, a similar energy of coupling has been obtained by others using analysis of the voltage dependence of activation,[8] rather than the Ca^{2+} dependence explored here. These results support the idea that the side chains of D50 and Q48 residues, as suggested by the crystal structure, interact and are involved in open state stabilization but this interaction does not play a major role in the stabilization of the open conformation in the absence (or low) extracellular Ca^{2+} concentrations.

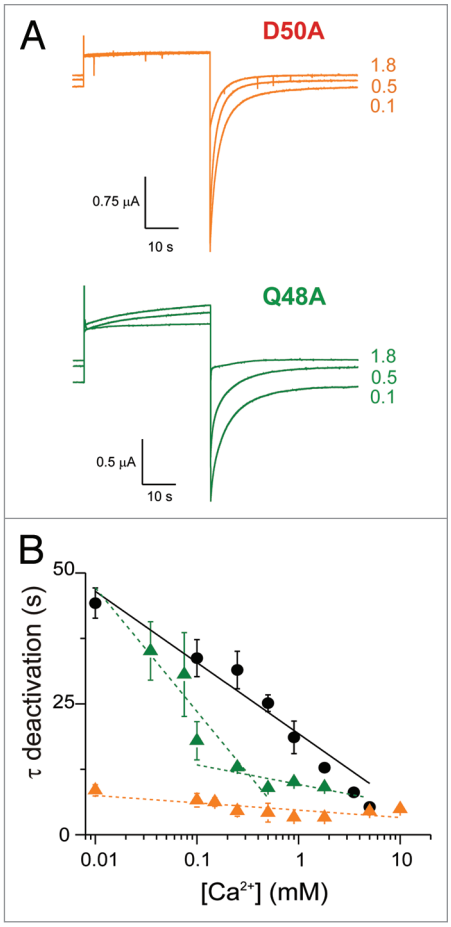

Figure 2. D50A mutation accelerates Ca^{2+}-induced closing of hCx26 hemichannels, while Q48A has a lesser effect, and only at the higher Ca^{2+} concentrations. (**A**) Representative current traces elicited by a pulse to 0 mV from a holding potential of -80 mV for an oocyte expressing D50A and Q48A mutant hemichannels at the indicated Ca^{2+} concentrations (mM). (**B**) Deactivation time constants of the corresponding tail currents at different Ca^{2+} concentrations for wild-type (black circles), D50A (orange triangles) and Q48A mutants (green triangles). The solid and dotted lines represent the best linear fits for wild-type and mutant channels, respectively. The data represent mean ± SEM of at least 3 independent measurements.

Methods

Channel expression and molecular biology

cDNA for hCx26 was purchased from Origene. Wild-type Cx26 was subcloned in the pGEM-HA vector (Promega) for expression in *Xenopus* oocytes. Mutations of hCx26 were produced with QuikChange II Site-Directed Mutagenesis Kits (Agilent Technologies). DNA sequencing performed at the NJMS Molecular Resource Facility confirmed the amino acid substitutions. Nhe1-linearized hCx26 wild-type and mutant DNAs were transcribed in vitro to cRNAs using the T7 Message Machine Kit (Ambion).

Electrophysiology

Electrophysiological data were collected using the 2-electrode voltage clamp technique. All recordings were made at room temperature (20–22 °C). The recording solutions contained (in mM) 118 NaCl, 2 KCl, 5 HEPES (pH = 7.4), with a range of divalent concentrations from 0.01–20. Currents from oocytes were recorded 1–3 d after cRNA injection using an OC-725C oocyte clamp (Warner Instruments). Currents were sampled at 2 kHz and low pass filtered at 0.2 kHz. Microelectrode resistances were between 0.1 and 1.2 MΩ when filled with 3 M KCl. All recordings were performed using agar bridges connecting bath and ground chambers.

Measurement of Ca^{2+} dose-response curves

Endogenous Cx38 expression was reduced by injections of antisense oligonucleotide against Cx38 (1 mg/ml; using the sequence from Ebihara et al.,[9]) 4 h after harvesting the oocytes. After

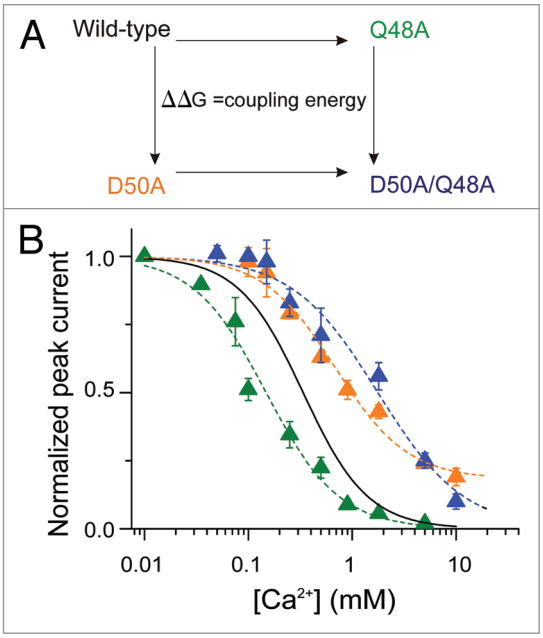

Figure 3. Mutant cycle analysis of K_D indicates that D50 and Q48 residues are thermodynamically coupled in the regulation of hCx26 hemichannels by Ca^{2+}. (**A**) Scheme for mutant cycle analysis of wild-type and mutant hemichannels. (**B**) Graph shows the $[Ca^{2+}]$ dose-response relations for oocytes expressing Q48A (green triangles) and D50A (orange triangles) mutants, and D50A/Q48A (blue triangles) double mutant hemichannels. The solid and dotted lines represent the best fits to the Hill equation for wild-type (from **Fig. 1B**) and mutant channels, respectively. The data represent mean ± SEM of at least 3 independent measurements.

1 d, the same oocytes were coinjected with 18–50 nl of cRNA (0.5–1 mg/ml) coding for hCx26 or for hCx26 mutants plus the Cx38 (1 mg/ml) antisense. Ca^{2+} and Mg^{2+} dose-response measurements were obtained by assessing the tail current peaks after reaching current saturation during a depolarizing pulse from -80 to 0 mV. Tail current measurements include the steady-state "holding" currents due to the opening of hemichannels at -80 mV induced by reduction of extracellular divalent concentrations. Deactivation time constants from tail currents were determined by fitting tail currents, up to 10 s after reaching steady-state, to exponential functions using Clampfit 11 software.

Mutant cycle analysis

Mutant cycle analysis was performed using the apparent affinities of Ca^{2+} derived from steady-state currents. Coupling energy (ΔΔG) was calculated as: $\Delta\Delta G = RT \ln(k_{[\text{wild-type}]} \times k_{[\text{double mutant}]} / k_{[\text{mutant1}]} \times k_{[\text{mutant 2}]})$ (**Eq. 2**) where R is the ideal gas constant and T is the absolute temperature. Significant coupling is indicated by any value above ± 0.5 kcal/mol.

Disclosure of Potential Conflicts of Interest

No potential conflicts of interest were disclosed.

Acknowledgments

This work was supported by National Institutes of Health/National Institute of General Medical Sciences (grant RO1-GM099490 to Contreras JE).

References

1. Willecke K, Eiberger J, Degen J, Eckardt D, Romualdi A, Güldenagel M, Deutsch U, Söhl G. Structural and functional diversity of connexin genes in the mouse and human genome. Biol Chem 2002; 383:725-37; PMID:12108537; http://dx.doi.org/10.1515/BC.2002.076
2. Thévenin AF, Kowal TJ, Fong JT, Kells RM, Fisher CG, Falk MM. Proteins and mechanisms regulating gap-junction assembly, internalization, and degradation. Physiology (Bethesda) 2013; 28:93-116; PMID:23455769; http://dx.doi.org/10.1152/physiol.00038.2012
3. Saez JC, Berthoud VM, Branes MC, Martinez AD, Beyer EC. Plasma membrane channels formed by connexins: their regulation and functions. Physiol Rev 2003; 83:1359-400; PMID:14506308
4. Xu J, Nicholson BJ. The role of connexins in ear and skin physiology - Functional insights from disease-associated mutations. Biochim Biophys Acta 2012; PMID:22796187
5. Martínez AD, Acuña R, Figueroa V, Maripillan J, Nicholson B. Gap-junction channels dysfunction in deafness and hearing loss. Antioxid Redox Signal 2009; 11:309-22; PMID:18837651; http://dx.doi.org/10.1089/ars.2008.2138
6. Lopez W, Gonzalez J, Liu Y, Harris AL, Contreras JE. Insights on the mechanisms of Ca(2+) regulation of connexin26 hemichannels revealed by human pathogenic mutations (D50N/Y). J Gen Physiol 2013; 142:23-35; PMID:23797420; http://dx.doi.org/10.1085/jgp.201210893
7. Maeda S, Nakagawa S, Suga M, Yamashita E, Oshima A, Fujiyoshi Y, Tsukihara T. Structure of the connexin 26 gap junction channel at 3.5 A resolution. Nature 2009; 458:597-602; PMID:19340074; http://dx.doi.org/10.1038/nature07869
8. Sanchez HA, Villone K, Srinivas M, Verselis VK. The D50N mutation and syndromic deafness: altered Cx26 hemichannel properties caused by effects on the pore and intersubunit interactions. J Gen Physiol 2013; 142:3-22; PMID:23797419; http://dx.doi.org/10.1085/jgp.201310962
9. Ebihara L. Xenopus connexin38 forms hemi-gap-junctional channels in the nonjunctional plasma membrane of Xenopus oocytes. Biophys J 1996; 71:742-8; PMID:8842212; http://dx.doi.org/10.1016/S0006-3495(96)79273-1